



## Effect of Differential Sizing of Coupled Beds on the Performance of Metal Hydride Based Sorption Cooling

Biju John Koshy<sup>1</sup>, G. Mohan<sup>1\*</sup>, M. Prakash Maiya<sup>2</sup>

<sup>1</sup> Centre for Computational Research in Clean Energy Technologies, Sree Chitra Thirunal College of Engineering, APJ Abdul Kalam Technological University, Thiruvananthapuram 695018, India.

<sup>2</sup> Refrigeration and Air Conditioning Lab, Indian Institute of Technology Madras, Chennai 600036, India.

\*Email: [mohan.g.menon@sctce.ac.in](mailto:mohan.g.menon@sctce.ac.in)

### Abstract

Hydrogen being the most abundant element in the universe has great potential towards decarbonisation at the point of usage. Metal hydride-based heat pumps/ refrigerators are getting increasing acceptance due to its environment friendliness and safety. These systems operate over a wide range of temperatures and pressures. The thermal performance of these systems depends mainly on the reaction kinetics of the alloy pairs. Difference in the reaction rates of the alloy pairs, causes a certain amount of hydride to go unutilized during cycling. Several studies have been reported on the sorption performance of these systems. However, studies on the effect of differential masses of alloy pairs used on the performance of these systems have not been reported. In the present study, numerical simulation of differently sized coupled beds based on the alloy pair of  $\text{LaNi}_{4.7}\text{Al}_{0.3}$  -  $\text{La}_{0.8}\text{Ce}_{0.2}\text{Ni}_5$  is carried out using COMSOL Multiphysics® commercial code. It is found that 12% increase in COP (0.28) is obtained for a cycle time of 260 s and mass ratio of 1.5. This corresponds to minimum alloy weight ensuring effective transfer of hydrogen with lowest disparity across HT-LT reactors.

**Keywords:** Metal Hydride, Cooling System, Simulation

### Nomenclature

T	temperature, K	$\varepsilon$	porosity
P	pressure, Pa	$\rho$	density, $\text{kg m}^{-3}$
c	concentration of hydride, $\text{mol m}^{-3}$	K	permeability, $\text{m}^2$
$C_p$	specific heat, $\text{J kg}^{-1} \text{K}^{-1}$	<i>Subscripts</i>	
E	activation energy, $\text{J mol}^{-1}$	a	absorption
R	universal gas constant, $8.314 \text{ J mol}^{-1} \text{K}^{-1}$	d	desorption
k	thermal conductivity, $\text{W m}^{-1} \text{K}^{-1}$	e	effective
C	material dependant constant, $\text{s}^{-1}$	eq	equilibrium
d	diameter, m	sat	saturation
COP	co-efficient of performance	s	solid
<i>Greek Letters</i>		A	reactor A
$\Delta H^0$	heat of formation, $\text{J kg}^{-1}$	B	reactor B
$\mu$	dynamic viscosity, $\text{kg m}^{-1} \text{s}^{-1}$	p	particle

## 1. Introduction

Hydrogen has great potential towards decarbonisation. Metal hydride based heating and cooling systems operate similar to conventional sorption systems. These are thermally driven systems which holds promise where waste heat (automobiles, solar or thermal) is available. Formation of hydride is an exothermic reaction while breaking of hydrogen bonds requires energy. A unique advantage of these systems is that any operational temperature can be met by suitably changing the alloy composition.

Nishizaki *et al.* [1] developed a model to analyse the performance of a metal hydride heat pump. The concept of sensible heating/cooling in the working cycle was introduced. The effect of operating parameters, thermo-physical properties and efficiency of heat exchange on the performance of coupled beds were presented. They concluded that for maximum performance of the system there should be flat plateau, low reactor heat capacities and efficient heat interaction. Muthukumar *et al.* [2] presented a review of metal hydride based heating and cooling systems. The operating principles of the various systems were presented and suggestions for the improvement of the coefficient of performance and specific cooling capacity were discussed.

Dantzer and Meunier [3] conducted an extensive study on the materials to be used in hydride chemical heat pumps. They studied three modes of applications namely, cooling, heat pump and heat transformer. Tyler *et al.* [4] developed a MATLAB toolbox, containing property database of over 300 hydrides. This allows a consideration of many combinations of alloy pairs for a given two hydride thermal systems. The performance of these pairs were also reported. They observed that hydride pairs having high hydriding enthalpies could achieve reasonable performance even with relatively low hydrogen transfer between them. Supper *et al.* [5] conducted experimental analysis on the reaction kinetics of various AB<sub>5</sub> alloys. They suggested using aluminium foam as a heat transfer enhancement method. The influence of extremely porous aluminium foam on the reaction kinetics was reported. The study was done for various bed thickness. According to Rusman and Dahari [6] addition of catalyst into the metal hydrides, alloying the metal hydrides and nano-structuring can be used to improve the absorption/ desorption properties of hydrogen. Sekhar and Muthukumar [7] conducted a numerical study to predict the performance of a single stage metal hydride-based heat transformer. The alloy pair of LaNi<sub>5</sub> and LaNi<sub>4.7</sub>Al<sub>0.3</sub> was considered for the analysis. Effect of operating temperatures namely, heat source, and heat output and heat rejection temperatures on the performance of the system was reported. The performance was found to be enhanced with increase in heat source temperature while it decreased with increase in heat output temperature. Effect of thermal conductivity and bed thickness on the performance were also reported.

Sharma and Kumar [8] analysed the reaction kinetics of certain La based metal hydrides to determine their suitability for cooling systems. The alloy pair of La<sub>0.8</sub>Ce<sub>0.2</sub>Ni<sub>5</sub> and LaNi<sub>4.7</sub>Al<sub>0.3</sub> showed the least cycle time. Sharma and Kumar [9] conducted a study on the properties of LaNi<sub>5-x</sub>Al<sub>x</sub> (x=0.3, 0.4). They calculated the enthalpy of formation and entropy of formation using vant' Hoff equation. The effects of Al content on the properties were analysed. Sharma and Kumar [10] also conducted a material characterisation of La<sub>0.9</sub>Ce<sub>0.1</sub>Ni<sub>5</sub>, La<sub>0.8</sub>Ce<sub>0.2</sub>Ni<sub>5</sub>, LaNi<sub>4.7</sub>Al<sub>0.3</sub> and LaNi<sub>4.6</sub>Al<sub>0.4</sub> to determine their suitability in metal hydride based cooling systems. Higher the pressure difference between the metal hydride beds, higher will be the cooling capacity in shorter cycle times. The main advantage of using (LaCe)Ni<sub>5</sub> and La(NiAl)<sub>5</sub> as low temperature and high temperature alloy respectively is that the low temperature alloy will desorb hydrogen at ambient temperature and desorb at lower temperatures down to -20C while the high temperature material can absorb hydrogen at ambient temperature and desorb at high temperatures. They rely on chemi-sorption.

The shape and size of the reactor plays an important role in the performance of the coupled beds. Many studies have been done based on metal hydride beds having a cylindrical geometry. Satheesh *et al.* [11] used fully implicit finite volume method to predict the heat and mass transfer characteristics between the coupled beds. They used transient, 2D mathematical model in an annular cylindrical configuration. Alloy pair of MmNi<sub>4.6</sub>Al<sub>0.4</sub> /MmNi<sub>4.6</sub>Fe<sub>0.4</sub> was used for analysis. Variation in hydrogen concentration, temperature distribution and equilibrium pressure were reported. The difference in cycle times for variable and constant wall temperature boundary conditions were approximately 5mins. The lowest refrigeration temperature observed was 269.1 K. Satheesh and Muthukumar [12] conducted the

performance analysis of a single stage metal hydride heat pump working with five different alloy pairs. The maximum COP of 0.66 was obtained. The highest specific cooling power obtained was 53.25 W/kg of total hydride mass. Satheesh and Muthukumar [13] also conducted a simulation of double stage metal hydride heat pump. They presented the variation in hydrogen concentrations, hydride equilibrium pressures and heat transferred for one complete cycle. For the given operating conditions they obtained a COP of 0.471 and SCP of 28.4W/kg of total hydride mass.

Malleswararao *et al.* [14] conducted 3D simulation of coupled Mg<sub>2</sub>Ni-LaNi<sub>5</sub> using COMSOL Multiphysics®, using an alloy pair of Mg<sub>2</sub>Ni and LaNi<sub>5</sub>. The thermodynamic compatibility criteria for the selection of metal hydride pairs was discussed. Malleswararao *et al.* [15] also conducted studies on long term and buffer modes of operations of a thermal energy storage system using the same alloy pair. Two interconnected cylindrical reactors were simulated using COMSOL Multiphysics®, to find the effect of heat source temperature on the thermal performance of system.

A few studies have been reported considering a reactor having a flat plate configuration. Weckerle *et al.* [16] conducted an experimental characterisation using metal hydride hydraalloy. They reported very short cycle time ( $t < 60$  s). Plate reactor concept is feasible for all metal hydride applications if the parasitic reactor mass can be reduced and external heat transfer can be increased. Weckerle *et al.* [17] conducted a numerical study and compared the results with the experimental work. Optimum thickness of the reactor for the application was found out. They considered an open cooling system. Kumar *et al.* [18] conducted studies on a metal hydride based year round comfort heating and cooling system for extreme climates. They presented the effects of system parameters on the performance of the system using the alloy pair of Zr<sub>0.82</sub>Mm<sub>0.09</sub>Ti<sub>0.09</sub>Fe<sub>1.4</sub>Cr<sub>0.6</sub> – LaNi<sub>4.6</sub>Al<sub>0.4</sub>. Capacity of absorption/desorption of hydrogen of the two metal hydrides considered were different. Alloy having lower sorption kinetics was considered the rate controlling factor. Differential masses of reactors were used to improve the performance. Maximum COP was obtained for a mass ratio of 1.83. Difference in the reaction rates of the alloy pairs can cause a certain amount of hydride to go unutilized during cycling or may lead to a pressure build up. The build-up of hydrogen pressure should be minimised. One way to achieve it is by using differential masses of two hydrides. Though several studies have been done on the thermal performance of these systems, the effect of differential masses of alloy pairs having similar absorption /desorption capacity on the system performance have not been reported. Numerical simulation of hydrogen transport between differently sized coupled beds based on the alloy pair of LaNi<sub>4.7</sub>Al<sub>0.3</sub> - La<sub>0.8</sub>Ce<sub>0.2</sub>Ni<sub>5</sub> was conducted.

## 2. Experimental/Analytical/Simulation

Figure 1, represents the schematic of a pair of metal hydride based flat plate reactors. The physical model consists of two flat plate reactors A and B of square cross section. The reactors are filled with the metal hydrides. Reactor A is filled with the high temperature alloy (HT alloy) and reactor B is filled with the low temperature alloy (LT alloy). They are connected together by means of a connecting pipe which has a control valve to regulate the flow of hydrogen between them.

The operating principle of a metal hydride based coupled beds is shown on the vant' Hoff plot (Figure 2). The refrigeration cycle consists of two heat and mass transfer processes (1-4 and 2-3) and two sensible heating/cooling processes (1-2 and 3-4). The cycle works between three temperature limits, high temperature ( $T_{high}$ ), intermediate temperature ( $T_m$ ) and low temperature ( $T_{low}$ ). Initially reactor A is considered to be fully hydrided and kept at temperature  $T_{high}$ . Reactor B is fully de-hydrided and kept at  $T_m$ . At this state there exist an equilibrium pressure difference between the two reactors. Equilibrium pressure of a reactor is a function of its temperature. Once the valve is opened, hydrogen gets desorbed from reactor A and travels towards reactor B, where it gets absorbed. While desorbing, the reactor A is supplied heat ( $Q_H$ ) using the heat transfer fluid to meet the required heat of reaction. While absorbing, the reactor B rejects heat ( $Q_{M,B}$ ) to the bed and heat transfer fluid. This process is called regeneration. The process continues for until certain amount of hydrogen is transferred between the reactors. Then, the valves are closed and both the reactors are sensibly cooled. Reactor A is cooled to  $T_m$  and reactor B is cooled to  $T_{low}$ . Once the valve is opened, hydrogen is desorbed from reactor B and gets absorbed in Reactor A. During desorption, the heat of reaction is taken from the bed and heat transfer fluid. This gives the refrigerating effect ( $Q_L$ ). This process is called refrigeration. Then both the reactors are

sensibly heated to initial temperatures. Air is taken as the heat transfer fluid. Air at the required temperature is passed over the flat plate reactors through ducts with an entry velocity of 3 m/s.

### 2.1. Physical model

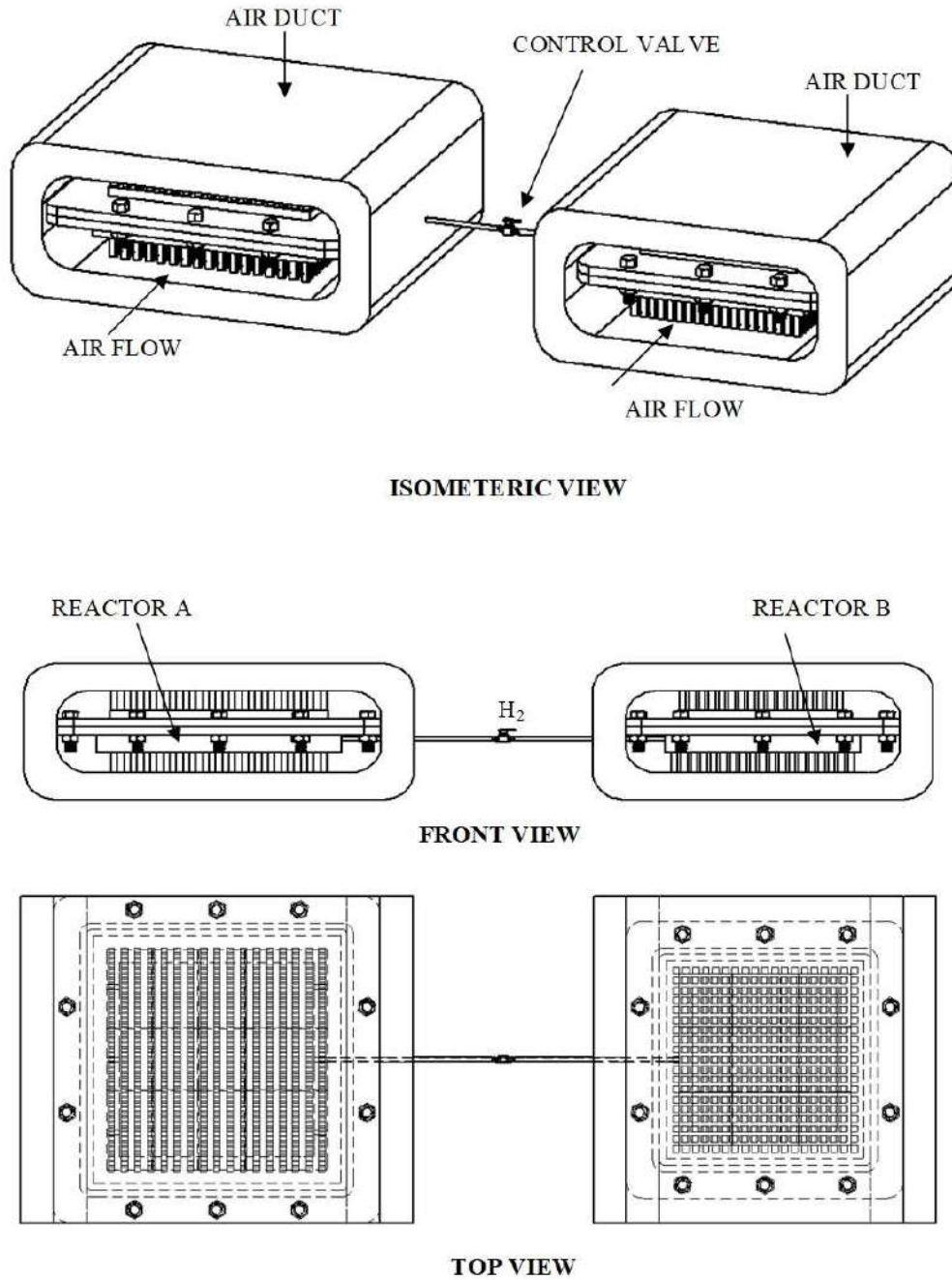


Figure 1. Physical model of metal hydride based coupled beds

The following assumptions were made to simplify the problem:

1. Effect of plateau slope and hysteresis have on sorption kinetics are neglected.
2. Thermo-physical properties are independent of the pressure, bed temperature and concentration.
3. Conduction is the prevalent mode of heat transfer within the bed.
4. Natural convection and radiation effects within the bed are neglected.
5. Hydride bed exhibits uniform porosity.
6. The reactors are insulated.

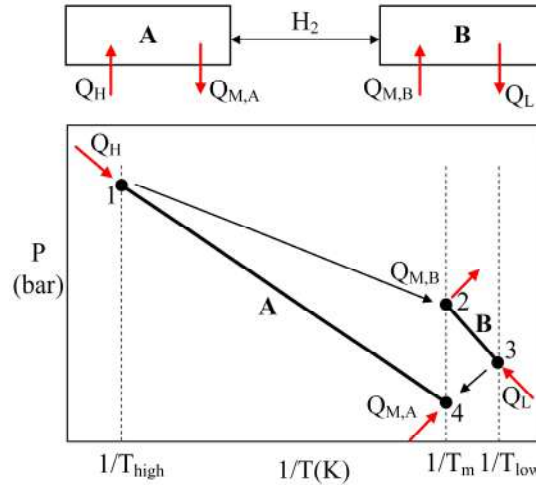


Figure 2. van't Hoff plot for single stage metal hydride based coupled beds

## 2.2. Problem formulation

### Mass balance of metal

Hydrogen entering the reactor bed gets converted to metal hydride with associated changes in density. Conservation of mass for the solid phase of reactor is expressed as

$$(1-\varepsilon)\frac{\partial \rho_s}{\partial t} = \dot{m} \quad (\text{Eq. 1})$$

$\dot{m}$  is the rate of gas absorbed

### Sorption kinetics

The amount of hydrogen absorbed is expressed as

$$\dot{m} = -C_a \exp\left(-\frac{E_a}{RT}\right) \ln\left(\frac{P}{P_{eq}}\right) (\rho_{sat} - \rho_s) \quad (\text{Eq. 2})$$

The amount of hydrogen desorbed per unit time and unit volume is expressed as

$$\dot{m} = -C_d \exp\left(-\frac{E_d}{RT}\right) \left(\frac{P-P_{eq}}{P_{eq}}\right) \rho_s \quad (\text{Eq. 3})$$

Equilibrium pressure is determined by van't Hoff relationship

$$\ln(P_{eq}) = A - \frac{B}{T} \quad (\text{Eq. 4})$$

A and B are van't Hoff constants

### Energy balance

Heat generated due to exothermic reaction causes associated spatial temperature imbalances within the bed. Energy conservation equation in the hydride is given by

$$(\rho C_p)_e \frac{\partial T}{\partial t} = k_e \frac{\partial}{\partial x} \left( \frac{\partial T}{\partial x} \right) + k_e \frac{\partial}{\partial y} \left( \frac{\partial T}{\partial y} \right) + k_e \frac{\partial}{\partial z} \left( \frac{\partial T}{\partial z} \right) - \dot{m} \Delta H^0 \quad (\text{Eq. 5})$$

The left hand term represents the heat of reaction and the right hand term includes the spatial variation of temperature.

### Momentum balance

Momentum balance for the flow of hydrogen can be expressed by the Brinkman equation (Eq. 6)

$$\begin{aligned} \frac{\partial}{\partial x} \left( \mu \frac{\partial u}{\partial x} \right) + \frac{\partial}{\partial y} \left( \mu \frac{\partial u}{\partial y} \right) + \frac{\partial}{\partial z} \left( \mu \frac{\partial u}{\partial z} \right) - \mu K u_x &= -\frac{\partial p}{\partial x} + F_x \\ \frac{\partial}{\partial x} \left( \mu \frac{\partial v}{\partial x} \right) + \frac{\partial}{\partial y} \left( \mu \frac{\partial v}{\partial y} \right) + \frac{\partial}{\partial z} \left( \mu \frac{\partial v}{\partial z} \right) - \mu K u_y &= -\frac{\partial p}{\partial y} + F_y \\ \frac{\partial}{\partial x} \left( \mu \frac{\partial w}{\partial x} \right) + \frac{\partial}{\partial y} \left( \mu \frac{\partial w}{\partial y} \right) + \frac{\partial}{\partial z} \left( \mu \frac{\partial w}{\partial z} \right) - \mu K u_z &= -\frac{\partial p}{\partial z} + F_z \end{aligned}$$

$F_x, F_y, F_z$  – Body forces per unit volume

Permeability (K) is calculated using the Kozeny-Carman equation

$$K = \frac{d_p^2 \varepsilon^3}{180 * (1 - \varepsilon)^2} \quad (\text{Eq. 7})$$

The performance of a metal hydride based coupled bed are characterized by the COP. It is defined as:

$$COP = \frac{Q_L}{Q_H} \quad (\text{Eq. 8})$$

$Q_L$  is the refrigeration effect and  $Q_H$  is the heat input.

## 2.3. Simulation methodology

The transfer of hydrogen between the reactors, as well as the heat interactions between the reactor beds and the heat transfer fluid, are predicted by solving the conservation equations for mass, momentum, and energy. In-built modules in COMSOL Multiphysics®, namely Transport of diluted species in porous media, Heat transport in porous media were used to implement the conservation of mass and energy of hydride beds. Air flow was simulated considering laminar flow. The size of the LT alloy was kept constant. The size of HT alloy was varied to vary the mass ratio of HT alloy to LT alloy from 1 to 2.5. The length along the direction of air flow was kept constant in all cases for both reactors. Table 1, shows the geometric parameters. The bed thickness of 4mm was kept constant. Physics-controlled mesh feature was used initially to generate the mesh elements, but to enhance the mesh quality, the element size was subsequently reduced. The model was solved using a segregated solver. The simulation was run for two cycles. The cycle time of 260 s is considered. It includes four processes denoted as a, b, c, and d: regeneration (120 s), sensible cooling (40 s), refrigeration (60 s), and sensible heating (40 s).

### 2.3.1 Validation of numerical model

For validation purpose, reactor geometry and operating conditions used by Satheesh *et al.* [11] is taken and simulation is done accordingly. The cycle time, bed thickness and thermo-physical properties are selected based on the conditions reported [11]. Figure 3, shows the variation of hydrogen concentration in both the reactors with time. The result obtained match reasonably well with the results reported in the literature for the alloy pair of  $\text{MmNi}_{4.6}\text{Al}_{0.4}$  and  $\text{MmNi}_{4.6}\text{Fe}_{0.4}$ . A small deviation between the results is due to the assumed values of reaction constants.

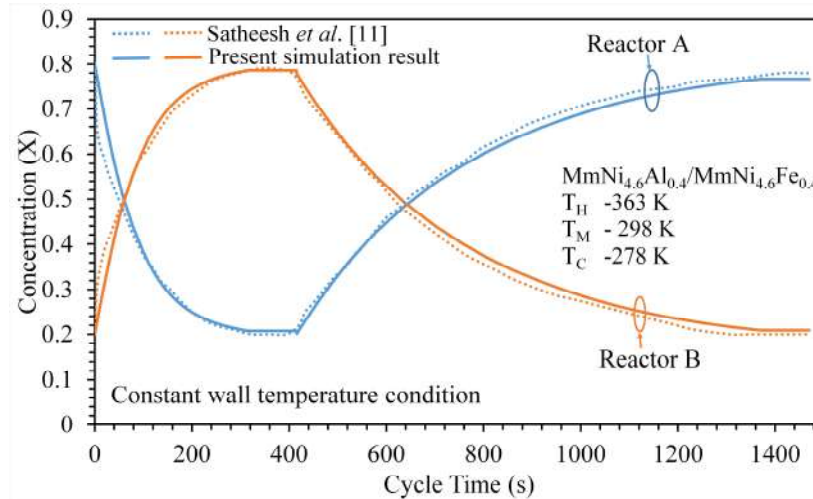


Figure 3. Validation of present simulation model with results of Satheesh *et al.* [11]

### 3. Results and discussion

The alloy pair of  $\text{LaNi}_{4.7}\text{Al}_{0.3}$  -  $\text{La}_{0.8}\text{Ce}_{0.2}\text{Ni}_5$  is considered for analysis. The alloy pair is well characterised, shows fast reaction kinetics and has good cycle life. Table 2, represents the operating conditions. The working range of the alloy pair matched the operating conditions. Table 3, represents the thermo-physical properties of alloy pair used for simulation.

Despite many applications proposed and studies conducted on metal hydride based systems [1-3, 8-18], very few have reached industrial development stage. This may be due to poor heat and mass transfer characteristics of metal hydride and high cycle time. Novelty can be made in the device design to reduce the cycle time to meet the required applications. Reactors with flat plate design [16-17], showed promising results for short cycle time. Another method to improve cycle time is to use differential masses for HT and LT alloys. However, studies on this is limited. Numerical simulation of hydrogen transport between flat plate coupled beds having differential masses is conducted in the present study.

Table 1. Geometric parameters values used in present simulation study

Geometric parameter	Values
Fin thickness (mm)	2
Inter-spacing between two fins (mm)	2
Height of fin (mm)	15
Length of connecting tube (mm)	150
Diameter of connecting pipe (mm)	6
Bed thickness (mm)	4

Table 2. Operating conditions considered in present simulation study

Operating conditions	Values
High temperature (K)	475
Intermediate temperature (K)	300
Low temperature (K)	283
Velocity of air at inlet of air domain (m/s)	3

Table 3. Thermo-physical properties of alloy pair.

Thermo-physical properties of alloy pair		La <sub>0.8</sub> Ce <sub>0.2</sub> Ni <sub>5</sub>	LaNi <sub>4.7</sub> Al <sub>0.3</sub>
Specific heat (J/kg K)		419	419
Thermal conductivity (W/m K)		1.3	1.3
Activation energy	Ea (J/mol)	21179.6	29210
	Ed (J/mol)	16420	28490
Density (kg/m <sup>3</sup> )		8200	8200
Porosity		0.5	0.5
Enthalpy of reaction (J/mol)		23800	34000
Entropy of reaction (J/mol K)		108	106.8
Reaction constants	Cd (1/s)	9.57	8.2
	Ca (1/s)	59.187	43.27

### 3.1. Hydrogenation of coupled beds during regeneration and refrigeration

Figure 4, represents the variation in hydrogen concentration in reactors A and B. During the regeneration process, the valve is opened, and as a result of the pressure differential, hydrogen is desorbed from the reactor A and absorbed by reactor B. As the mass ratio ( $M_{HT}/M_{LT}$ ) increases, more amount of hydrogen is desorbed from reactor A and absorbed in reactor B. The process continues for 120 s. During sensible cooling, the valve is closed and there is no transfer of hydrogen between the reactors. After this process, the equilibrium pressure in reactor B will be much higher than that in reactor A. At 160 s, the valve is opened and due to the pressure differential hydrogen gets desorbed from reactor B and gets absorbed in reactor A. The cooling effect is obtained during this process from LT side. Valve is closed and the reactors are heating to their initial temperatures. The gas pressure is continuously evolving so the pressure differential which is the driving potential changes with time. This leads to difference in sorption rates for different mass ratios at a given time. Figures 5a and 5b, represent the surface temperature of HT and LT sides for a mass ratio of 1.5 at different time durations. As shown in Figure 5a, at a time duration of 10 s, the heat of reaction is supplied by the heat transfer fluid. The inlet air temperature is at 475 K while the minimum bed temperature is 466 K. At 130 s the system undergoes cooling. The inlet air temperature is kept at 300 K. At 170 s, hydrogen is desorbed from reactor B and absorbed in reactor A. The reactor is cooled using air at 300 K. After refrigeration, the reactor is heated to initial conditions. As shown in Figure 5b, at a time duration of 10 s, hydrogen is absorbed in reactor B. Air at 30 K is used to cool the reactor to improve absorption. At 130 s, the reactor is sensibly cooled by air at 283 K. The minimum temperature of reactor reaches 305 K. At 170 s, the maximum refrigeration effect is achieved and a minimum bed temperature of 279 K is obtained. After refrigeration, the reactor is sensibly heated to initial conditions.

Figure 6a, represents the variation of bed temperatures for different mass ratios with time. The temperature variation during regeneration in reactor A is shown in Figure 6b. The heat of reaction is supplied by the heat transfer fluid. The heat input is at 475 K. As a result of this high heat input, the temperature of reactor A increases. The temperature rise depends on the initial reaction rate. The temperature increases and tends to attain the air temperature. The temperature of reactor B increases while absorbing hydrogen and gradually approach the air temperature. The rise in temperature is due to the low thermal conductivity of hydride bed. The temperature variation in reactor B during refrigeration is shown in Figure 6c. The temperature of the reactor suddenly drops and gradually attains the heat transfer fluid temperature. This drop depends on the initial reaction rate. The bed temperature depends on the amount of hydrogen desorbed and amount of heat transferred by the heat transfer fluid. The amount of hydrogen desorbed depends on the pressure differential between the reactors. As the pressure is continuously evolving, the driving potential fluctuates which contributes to the rate of change of bed temperatures for different mass ratios.



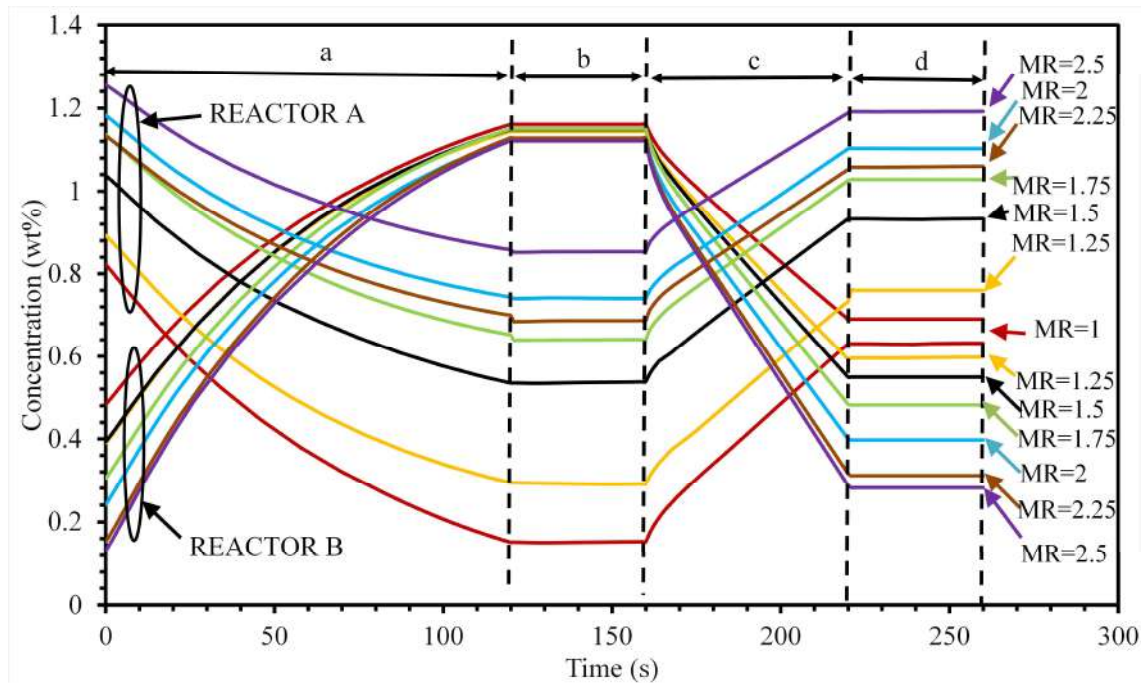


Figure 4. Effect of mass ratio ( $M_{HT}/M_{LT}$ ) on hydrogen concentration.  
 $T_{high}=475$  K,  $T_m=283$  K and  $T_{low}=283$  K  
 (a- Regeneration, b- Sensible Cooling, c- Refrigeration, d- Sensible heating)

Figure 7a, shows the hydrogen pressure in the metal hydride based coupled beds across a cycle. For regeneration and refrigeration, the hydrogen pressure in both reactors is similar to the equilibrium pressure of desorbing alloy. Equilibrium pressure is a function of the bed temperature. Figure 7b, shows the hydrogen pressure during desorption. As pressure differential increases, more hydrogen will be desorbed from reactor A. As more hydrogen is desorbed, it will have a negative effect on the driving potential but will enhance absorption in reactor B. the hydrogen pressure is continuously evolving so the driving potential also changes with time. Figure 7c, shows the hydrogen pressure during refrigeration. The maximum pressure differential is observed at the start of reaction and it gets reduced as hydrogen is desorbed from the reactor bed. The pressure differential increases as MR increases at the start of reaction. The increment in driving potential decreases after  $MR=2.25$ . Further increase in MR, will only result in a small increment in the amount of hydrogen desorbed from reactor B.

### 3.2. Effect of mass ratio on the performance of coupled bed

Figure 8, shows the variation of heat input and the refrigeration effect obtained for different mass ratios ratio ( $M_{HT}/M_{LT}$ ). As the mass ratio is increased, the amount of hydrogen transferred between the reactors increases. The increase in the amount of cycled hydrogen increases the refrigeration effect and heat input. Figure 9, represents the effect of mass ratio on the COP of the system. For a mass ratio  $MR=1.5$  to  $MR=2.25$ , the increase in refrigeration effect dominates the increase in heat input. This region shows maximum COP. The difference between the mass of hydrogen desorbed in reactor B and absorbed in reactor A is least for this range of mass ratios. After that, the mass of hydrogen transferred does not increase but the heat input increases which leads to a reduction in COP. The maximum COP obtained is 0.28.

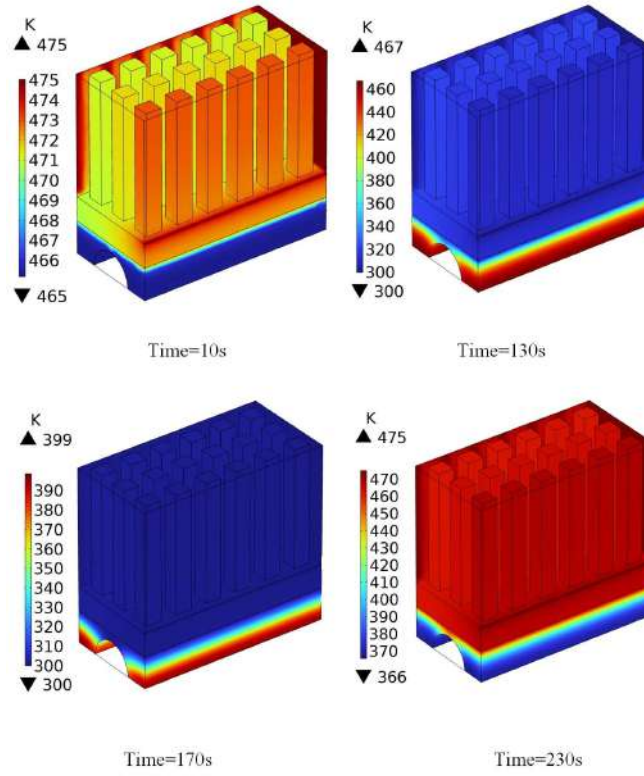


Figure 5a. Spatial variation of surface temperature of HT side at different time intervals.  
 $MR=1.5$ .  $T_{high}=475$  K,  $T_m=283$  K and  $T_{low}=283$  K

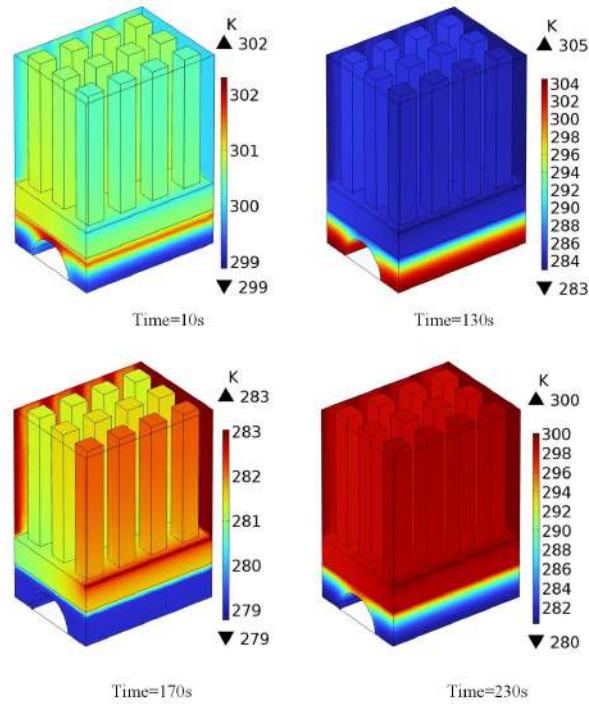


Figure 5b. Spatial variation of surface temperature of LT side at different time intervals.  
 $MR=1.5$ .  $T_{high}=475$  K,  $T_m=283$  K and  $T_{low}=283$  K.

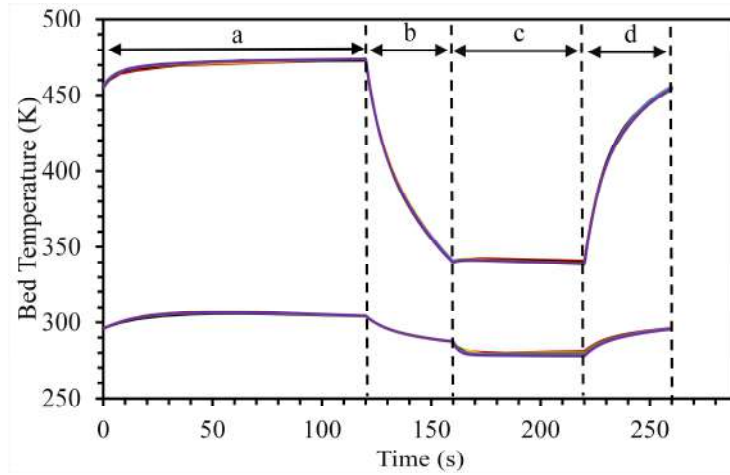


Figure 6a. Effect of mass ratio ( $MR=M_{HT}/M_{LT}$ ) on the average bed temperature at different time intervals.  $T_{high}=475$  K,  $T_m=283$  K and  $T_{low}=283$  K.

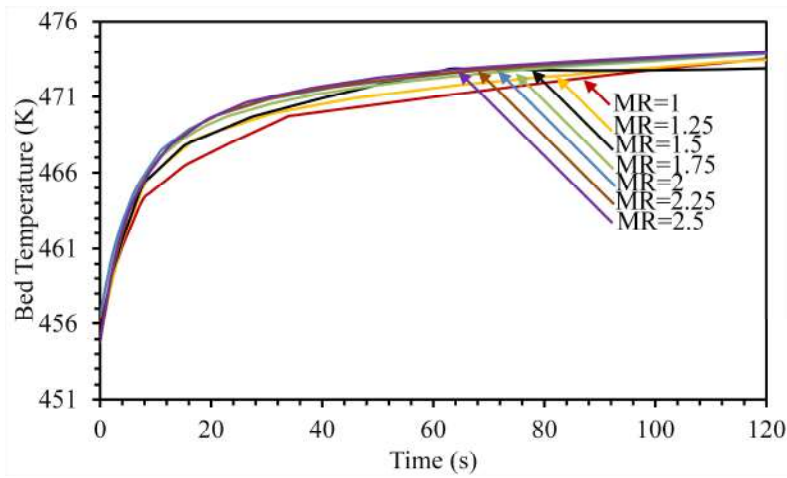


Figure 6b. Effect of mass ratio ( $MR=M_{HT}/M_{LT}$ ) on the average bed temperature of reactor A during Regeneration at different time intervals.  $T_{high}=475$  K,  $T_m=283$  K and  $T_{low}=283$  K.

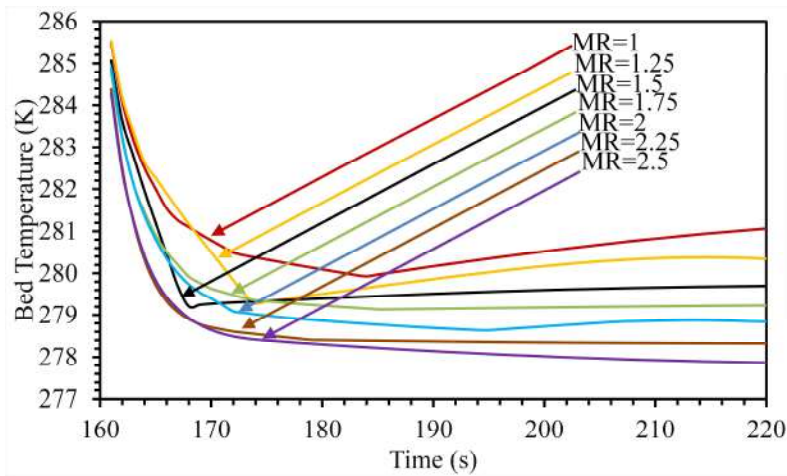


Figure 6c. Effect of mass ratio ( $MR=M_{HT}/M_{LT}$ ) on the average bed temperature of reactor B during Refrigeration at different time intervals.  $T_{high}=475$  K,  $T_m=283$  K and  $T_{low}=283$  K.

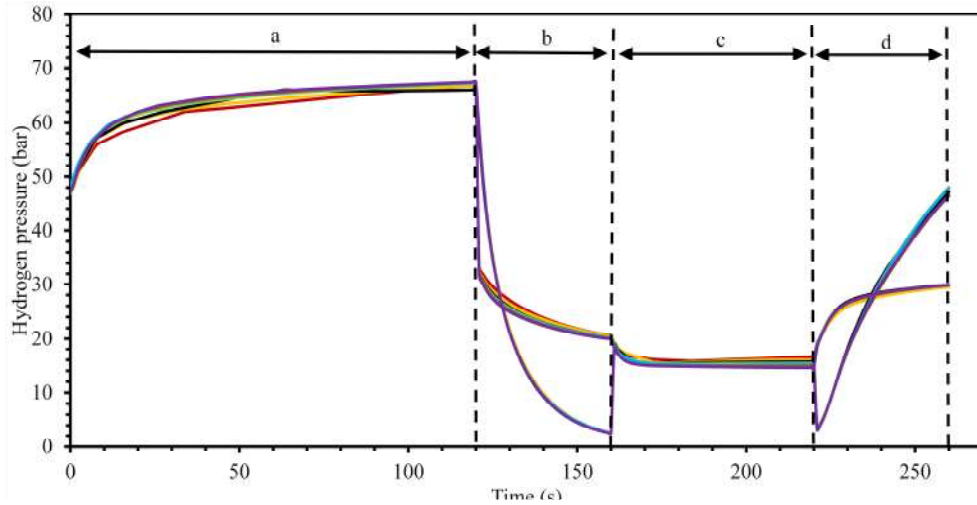


Figure 7a. Effect of mass ratio ( $MR=M_{HT}/M_{LT}$ ) on hydrogen pressure at different time intervals.  $T_{high}=475$  K,  $T_m=283$  K and  $T_{low}=283$  K.

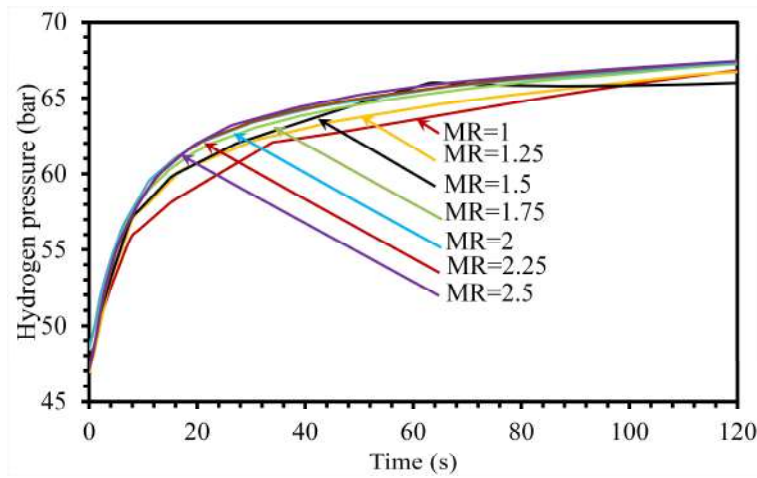


Figure 7b. Effect of mass ratio ( $MR=M_{HT}/M_{LT}$ ) on the hydrogen pressure in reactor A during Regeneration at different time intervals.  $T_{high}=475$  K,  $T_m=283$  K and  $T_{low}=283$  K.

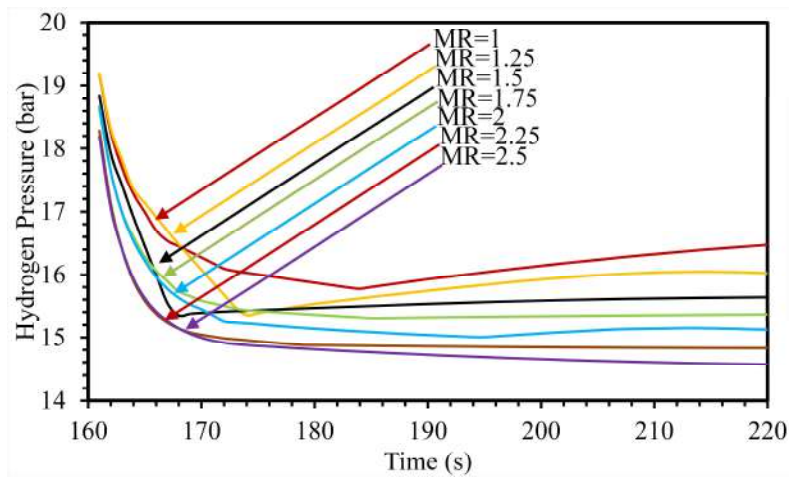


Figure 7c. Effect of mass ratio ( $MR=M_{HT}/M_{LT}$ ) on the hydrogen pressure in reactor B during Refrigeration at different time intervals.  $T_{high}=475$  K,  $T_m=283$  K and  $T_{low}=283$  K.

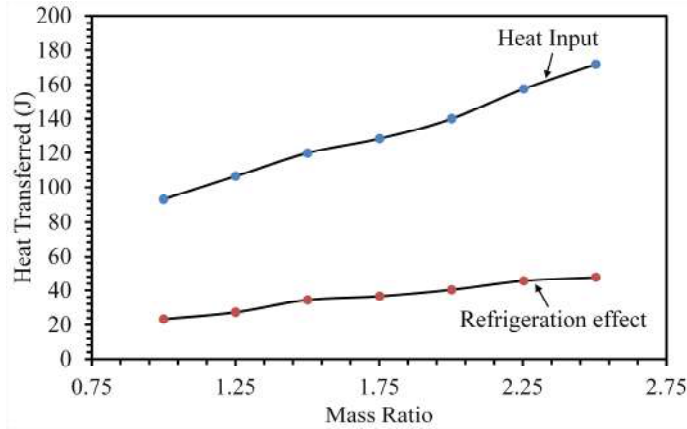


Figure 8. Effect of mass ratio ( $M_{HT}/M_{LT}$ ) on the heat input and refrigeration effect.  $T_{high}=475$  K,  $T_m=283$  K and  $T_{low}=283$  K.

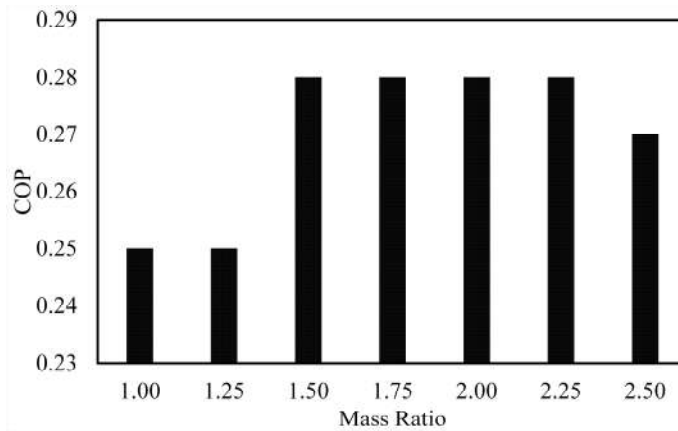


Figure 9. Effect of mass ratio ( $M_{HT}/M_{LT}$ ) on the COP.  $T_{high}=475$  K,  $T_m=283$  K and  $T_{low}=283$  K.

#### 4. Conclusions

Numerical simulation of a metal hydride based coupled bed with the alloy pair of  $LaNi_{4.7}Al_{0.3}$  -  $La_{0.8}Ce_{0.2}Ni_5$  is conducted using COMSOL Multiphysics® commercial code. The effect of differential masses of HT and LT alloys on the performance of the system is studied. It is found that 12% increase in COP (0.28) is obtained for a cycle time of 260 s and mass ratio of 1.5. This corresponds to minimum alloy weight ensuring effective transfer of hydrogen with lowest disparity across HT-LT reactors.

#### Acknowledgments

This study is supported by the Department of Science and Technology, Government of India under MECSP 2017 scheme. The suggestions rendered by Dr. K. Balasubramanian, NFTDC Hyderabad is greatly acknowledged.

## References

1. T. Nishizaki, K. Miyamoto and K. Yoshida, Coefficients of performance of hydride heat pumps, *Journal of less common materials* 89 (1983) 559-566.
2. P. Muthukumar and M. Groll, Metal hydride based heating and cooling systems: A review, *International Journal of hydrogen energy* 35 (2010) 23817-3831.
3. P. Dantzer and F. Meunier, What materials to use in hydride chemical heat pumps, *Material Science forum* Vol 31 (1988).
4. Tyler G. Voskuilen, Essene L. Waters and Timothee L. Pourpoint, A comprehensive approach for alloy selection in metal hydride thermal systems, *International Journal of Hydrogen energy* 39(2014) 13240-13254.
5. W. Supper, M. Groll and U. Mayer, Reaction kinetics in metal hydride reaction beds with improved heat and mass transfer, *Journal of Less –Common Metals* 104 (1984) 279-286.
6. N. A. A Rusman and M. Dahari, A review on the current progress of metal hydrides material for solid-state hydrogen storage application, *International Journal of hydrogen Energy* (2016) 1-19.
7. B. Satya Sekhar and P. Muthukumar, Performance Analysis of a Metal Hydride Based Heat Transformer, *International Energy Journal* 13 (2012)29-44.
8. Vinod Kumar Sharma and E. Anil Kumar, Measurement and analysis of reaction kinetics of La based hydride pairs suitable for metal hydride based cooling systems, *International Journal of hydrogen energy* (2014)1-13.
9. Vinod Kumar Sharma and E. Anil Kumar, Effect of measurement parameters on thermodynamic properties of La-based metal hydrides, *International Journal of Hydrogen Energy* 39 (2014) 5888-5898.
10. Vinod Kumar Sharma and E. Anil Kumar, Studies on La based intermetallic hydrides to determine their suitability in metal hydride based cooling systems, *Intermetallics* 57(2015) 60-67.
11. A. Satheesh, P. Muthukumar and Anupam Dewan, Computational study of metal hydride cooling system, *International Journal of Hydrogen Energy* 34 (2009) 3164-3172.
12. A. Satheesh and P. Muthukumar, Performance investigations of a single stage metal hydride heat pump, *International Journal of Hydrogen Energy* 35 (2010) 6950-6958.
13. A. Satheesh and P. Muthukumar, Simulation of double stage double effect metal hydride heat pump, *International Journal of Hydrogen Energy* 35 (2010) 1474-1484.
14. K. Malleswararao, N. Aswin, S. Srinivasa Murthy and Pradip Dutta, Performance prediction of a coupled metal hydride based thermal energy storage system, *International Journal of Hydrogen Energy* 45 (2020) 16239-16253.
15. K. Malleswararao, N. Aswin, S. Srinivasa Murthy and Pradip Dutta, Studies on long-term and buffer modes of operations of a thermal energy storage system using coupled metal hydrides, *Energy* 258 (2022) 124868.
16. C. Weckerle, I. Burger and M. Linder, Novel reactor design for metal hydride cooling systems, *International Journal of Hydrogen Energy* (2017) 8063-8074.
17. C. Weckerle, I. Burger and M. Linder, Numerical optimization of a plate reactor for a metal hydride open cooling system, *International Journal of Hydrogen Energy* (2019) 16862-16876.
18. Sachin Kumar, Pradip Dutta, S. Srinivasa Murthy, Yu. I. Aristov, L. Gordeeva, T. X. Li and R. Z. Wang, Studies on a metal hydride based year round comfort heating and cooling system for extreme climates, *Energy and Buildings* 244 (2021) 111042.